Astron. Astrophys. 358, 701–707 (2000)

ASTRONOMY AND ASTROPHYSICS

The morphology of clumps in molecular clouds excited by radiation from HH objects

A.C. Raga[1] **and D.A. Williams**[2]

[1] Instituto de Astronomía, UNAM, Ap. 70-264, 04510 D.F., México (raga@astroscu.unam.mx)
[2] Department of Physics and Astronomy, University College London, Gower Street, London WC1E 6BT, UK (daw@star.ucl.ac.uk)

Received 10 November 1999 / Accepted 12 April 2000

Abstract. We have investigated the influence of the radiation field from a Herbig-Haro object on a spherical clump, as the HH object passes by the clump. We have included a limited chemistry, and show column density maps of HCO^+ and NH_3 to represent the morphology of the predicted emission regions. The morphology is sensitive both to the orientation of the line of sight with respect to the HH trajectory and the clump, and to the extinction of the clump. Emission regions may appear bar-like, arc-like, or clump-like. The fractional abundances within these structures are observationally significant. However, the clump is not significantly heated by the radiation, and no clump evaporation occurs during the passage of the HH object for cases where the trajectory does not impact on the clump.

Key words: hydrodynamics – molecular processes – ISM: clouds – ISM: Herbig-Haro objects

1. Introduction

There is considerable evidence for the existence of small, localised regions (of a size about 0.1 pc) of enhanced molecular emission associated with HH objects (Rudolph & Welch 1988; Torrelles et al. 1992, 1993; Girart et al. 1994, 1998). The emission enhancements were first detected in NH_3 and HCO^+, and work in progress (Girart et al., in preparation) has demonstrated that there is also emission from several other species, including CH_3OH. These emission regions are cool and quiescent, and have velocities that are typical of the molecular cloud into which the HH shock is penetrating, rather than of the HH object itself. The material generating the molecular emission is evidently unshocked.

Girart et al. (1994) proposed that the emission regions are affected by the radiation field generated by the HH shock, so that molecules are liberated from icy mantles on dust grains in a density enhancement within the molecular cloud. The radiation will also promote a photochemistry within this region. Subsequently, theoretical studies by Taylor & Williams (1996) investigated the production of NH_3 and HCO^+ by such a mechanism, and their conclusions supported the Girart et al. proposal. Viti & Williams (1999) have extended the chemistry used by Taylor and Williams, and treated the development of the pre-existing clump more realistically. They predict that a variety of species should be detectable, including the CH_3OH detected by Girart et al.

However, these theoretical studies have investigated the time dependence of the chemistry in a *static* configuration, i. e., the source of the radiation affecting the clump is fixed in space relative to the clump. In reality, of course, the HH object will pass by the clump on a timescale that is comparable with chemical timescales within the clump. Therefore, it is necessary to develop a model in which the velocity of the HH object is included. This motion of the HH object then generates a radiation field intensity that is time-dependent, allowing for both the shock speed and the distance of the HH object from the clump. This paper describes the results of such a model. The clump is taken to be spherical, and located at a specified distance from the trajectory of the HH object. Details of the model are presented in Sect. 2. The time dependent chemical response within the clump is described in Sect. 3, and the morphology of the predicted emission regions is discussed in Sect. 4, with reference to the observed morphologies for HCO^+ in the case of HH80N (Girart et al. 1998) and for NH_3 in the case of HH80N (Girart et al. 1998) and HH1 (Torrelles et al. 1993).

2. The model

The geometry of the model is illustrated in Fig. 1. The radiation source S travels with speed v on a path with impact parameter b_0 to the centre of the clump. The clump is taken to be spherical, with initially uniform number density and temperature, n_c and T_c, respectively, and is sufficiently small that self gravity is negligible. The column density along a radius of the clump is specified in terms of the visual extinction, A_{vc},(assuming a standard gas-dust ratio). The clump is embedded in an ambient medium of number density and temperature, n_0 and T_0, respectively.

It is assumed that pressure balance exists between the clump and the ambient medium. This requirement may imply somewhat unphysical parameters for the ambient medium. However, since we are primarily concerned with the chemical development within the clump this is not a serious defect. The ini-

Send offprint requests to: A.C. Raga

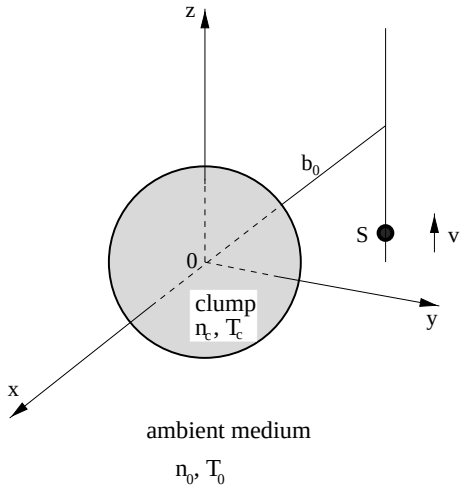

Fig. 1. The clump, assumed to be spherical, is located at the origin of coordinates, O. The radiation source travels with speed v along a line parallel to the z-axis. This line cuts the (x, y) plane at $(-b_0, 0)$.

tial chemical condition of the clump is chosen to represent an evolved density enhancement of the cloud in which most of the material is molecular and in which substantial ice mantles have been deposited on the dust grains. In the less dense and warmer ambient medium there are no ice mantles, consistent with the observed onset of ice at critical values of A_v (e.g., Chiar et al. 1995). The initial values of the physical and chemical parameters that have been used for both the clump and the ambient medium are given in Table 1.

We model the HH object as a photon source which travels at a constant velocity v in a trajectory parallel to the z-axis (see Fig. 1). The radiation field of the source is dependent on the shock velocity and can be approximated by:

$$S_{HH} = n_0 v \left(\frac{v}{100\,\mathrm{km\,s^{-1}}}\right)^2 \pi\, {r_{HH}}^2\,, \qquad (1)$$

where v is the bow shock speed, r_{HH} is the radius and S_{HH} is the total number of photons emitted per unit time by the HH object (Raga & Wang 1994). This value is similar to that derived by Wolfire & Königl (1991, 1993).

In order to illustrate the kind of values obtained for the radiative flux, we note the following. For the parameters chosen for the models discussed in the present paper (see Table 1), Eq. (1) gives $S_{HH} = 2.51 \times 10^{43}$ s^{-1}. For the point of closest approach of the HH object to the surface of the clump (at which the HH object is at a distance of 1.5×10^{17} cm from the near side of the clump), the flux impinging on the surface of the clump has a value of 8.9×10^7 cm^{-2} s^{-1}, corresponding to approximately 9% of the mean interstellar field.

The dynamical, thermal, and chemical evolution of the clump is then evaluated using the "yguazú" three dimensional hydrodynamical code (Raga et al. 1999) coupled with a very limited chemical network that is intended to model the clump chemistry of NH_3 and HCO^+. The "yguazú" code integrates the 3D gasdynamic equations with the "flux vector splitting" algorithm of Van Leer (1982), and simultaneously solves the radiative transfer equation as well as equations for a number of atomic/ionic or molecular species (see Raga et al. 1999). The main heating source is assumed to be photoelectric emission from dust, and a value of 2.5×10^{-26} erg s^{-1} per H atom has been adopted for heating by the canonical interstellar radiation field (Bakes & Tielens 1994). This heating rate must then be scaled by the actual radiation intensity at the clump, in interstellar units, for any given geometrical configuration. Cooling within the clump is through O atom fine structure (Launay & Roueff 1977; Monteiro & Flower 1987) and CO rotational excitation (McKee et al. 1982).

The very limited chemical network is shown in Table 2. The rate coefficients are taken from the UMIST data base (Millar et al. 1997). This chemistry is driven by the HH radiation field acting on the species H_2O, NH_3, and CO that are assumed to be

Table 1. Initial values of physical and chemical parameters

Physical parameters	Model 1 (Model 2)[1]
Impact parameter b_0 (cm)	2.5×10^{17}
Clump number density n_c (cm^{-3})	10^5 (2×10^4)
Clump temperature T_c (K)	10
Clump radius (cm)	10^{17}
Clump radius visual extinction (magnitudes)	5 (1)
Ambient number density n_0 (cm^{-3})	10^3
Ambient temperature T_0 (K)	10^3 (200)
HH velocity v (km s^{-1})	200
HH radius r_{HH} (cm)	10^{16}
Chemical parameters	
Desorption efficiency	0.003
Fractional Abundances: clump; ambient	
$H_{2\,\mathrm{gas}}$	0.5; 0.5
H_2O_{gas}	0.0; 0.0
H_2O_{ice}	10^{-4}; 0.0
CO_{gas}	10^{-4}; 10^{-4}
CO_{ice}	10^{-4}; 0.0
$NH_{3,\mathrm{gas}}$	0.0; 0.0
$NH_{3,\mathrm{ice}}$	10^{-5}; 0.0
C_{gas}	10^{-6}; 10^{-6}
$C^+{}_{\mathrm{gas}}$	10^{-7}; 10^{-7}

[1] the parameters for Model 2 are given in parentheses when different from the Model 1 parameters

Table 2. The chemical network

1.	$\mathrm{CO} + \mathrm{h}\nu \rightarrow \mathrm{C} + \mathrm{O}$
2.	$\mathrm{C} + \mathrm{h}\nu \rightarrow \mathrm{C}^+ + \mathrm{e}$
3.	$\mathrm{H_2O{-}d} + \mathrm{h}\nu \rightarrow \mathrm{H_2O} + \mathrm{d}$
4a.	$\mathrm{C}^+ + \mathrm{H_2O} \rightarrow \mathrm{HCO}^+$
4b.	$\mathrm{C}^+ + \mathrm{H_2O} \rightarrow \mathrm{HOC}^+ \rightarrow \mathrm{HCO}^+$
5.	$\mathrm{HCO}^+ + \mathrm{H_2O} \rightarrow \mathrm{CO} + \mathrm{H_3O}^+$
6.	$\mathrm{HCO}^+ + \mathrm{C} \rightarrow \mathrm{CO} + \mathrm{CH}^+$
7.	$\mathrm{H_2O} + \mathrm{h}\nu \rightarrow$ products
8.	$\mathrm{NH_3{-}d} + \mathrm{h}\nu \rightarrow \mathrm{NH_3} + \mathrm{d}$
9.	$\mathrm{NH_3} + \mathrm{h}\nu \rightarrow$ products
10.	$\mathrm{CO{-}d} + \mathrm{h}\nu \rightarrow \mathrm{CO} + \mathrm{d}$

d denotes dust grains

photodesorbed from the icy mantles on the dust grains. Source terms to represent this desorption are introduced into the rate equations. The source term for H_2O is calculated by assuming that UV photons can desorb H_2O molecules, with an efficiency of $\eta \approx 0.003$ molecules per photon (as obtained from laboratory measurements by Westley et al. 1995). For a radiation field intensity of G times the interstellar radiation field, then the H_2O source term may be written as

$$S(\mathrm{H_2O}) = \eta\, G \exp(-2.5 A_v) \times 10^{-12}\,, \tag{2}$$

in units of molecules per second per H nucleus. We further assume

$$S(\mathrm{NH_3}) = S(\mathrm{H_2O})\,. \tag{3}$$

However, CO is likely to be less tightly bound in the ice, and various mechanisms for CO desorption have been proposed (e.g. Allen and Robinson 1975; d'Hendecourt et al. 1982; Léger et al. 1985; Willacy & Williams 1993). Some of these operate in the infrared (e.g., Dzegilenko & Herbst 1994, 1995; Dzegilenko et al. 1995). Therefore, we drop the exponential in Eq. (3) and write

$$S(\mathrm{CO}) = \eta\, G \times 10^{-12}\,, \tag{4}$$

in molecules per second per H nucleus.

3. Results

Selected results are illustrated in Figs. 2–9. We discuss first the morphology of the predicted images for the two species for which the limited chemical network was designed.

3.1. Model 1 – HCO$^+$

Fig. 2 shows the HCO^+ fractional abundance at various times in a plane of the clump defined by the path of the HH object and the centre of the clump (the $y = 0$ plane). The abundances are presented at four times during the passage of the radiation source by the clump. At the earliest time shown (400 years) the source is at $z = -4 \times 10^{17}$ cm, $x = -2 \times 10^{17}$ cm, and moves parallel to the z-axis. At later times the position of the source is indicated in the figure. Fig. 2 shows that the HCO^+ in the $y = 0$ plane is produced in an arc around the edge of the clump. The position of this arc follows the direction to the source, but lags behind owing to the finite chemical timescale associated with forming the HCO^+. The abundance of the molecule therefore continues to rise even when the radiation source has begun to move away from the clump. The fractional abundances obtained for HCO^+ are high, more than 10^{-6} at the maximum. The position and the abundance reflect the production of both C^+ and H_2O in those parts of the clump closest to the radiation source.

Abundances on all planes $y = const$ have been calculated, so that column densities for any orientation of the clump and line of sight may be obtained. These column density maps give a good indication of the predicted morphology of the clump, for any orientation, because the thermal and dynamical effects of the heating of the clump have been determined to be negligible and within the space and velocity resolution of the numerical techniques adopted. For example, the temperature change in the surface layers when the radiation source is at closest approach is merely one or two degrees K. Fig. 3 therefore indicates the expected morphology of the observed clump in the case of Model 1, with the centre of the clump directly in front of the line of motion of the HH object. The apparent size of the HCO^+ emitting region is somewhat less than the size of the clump in which the HCO^+ is generated. The HCO^+ emission is most intense after the HH object has passed by the clump, and the position of the HCO^+ emitting region follows the motion of the HH object.

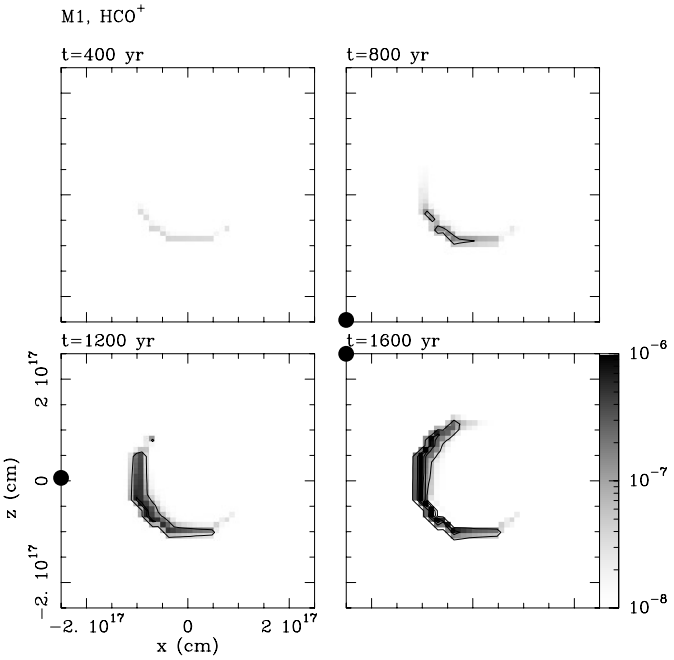

Fig. 2. The fractional abundance of HCO^+ in the $y = 0$ plane of the clump, at times $t = 400$, 800, 1200, and 1600 years, for Model 1. The position of the HH object is indicated by the marker on the z-axis. At time $t = 0$, the position of the clump is at $z = -4 \times 10^{17}$ cm. The greyscale is logarithmic, and the contours correspond to steps of 5×10^{-7} in the fractional abundance, the lowest contour corresponding to an abundance of 10^{-7}.

Fig. 4 shows the appearance of the clump in HCO^+ emission when viewed from a direction perpendicular to the plane containing the line of motion of the source and the clump centre, so that the path of the HH object appears to one side of the clump. The morphology in this orientation is similar to the fractional density plot in Fig. 2. The HCO^+ generates an arc of emission appearing on the side of the clump nearest to, but lagging behind, the motion of the HH object.

The most intense emission occurs when the HH object is closest to or just past the clump, and column densities around 10^{15} cm^{-2} are predicted. The peak column densities (as a function of time) corresponding to the maps shown in Fig. 4 are listed in Table 3.

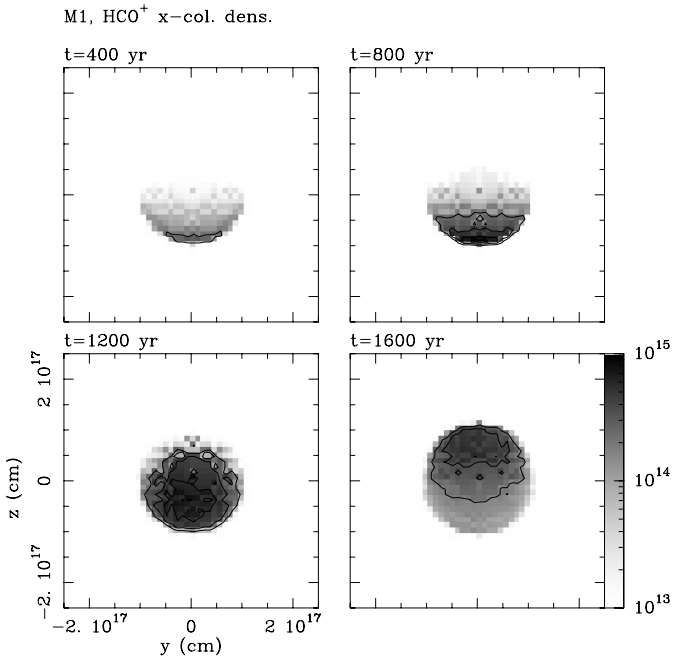

Fig. 3. Column densities (cm^{-2}) of HCO^+ through the clump integrated along lines parallel to the x-axis, at four times, for Model 1. In this orientation, the trajectory of the HH object is directly behind the centre of the clump. The greyscale is logarithmic, and the contours correspond to steps of 2×10^{14} cm^{-2}.

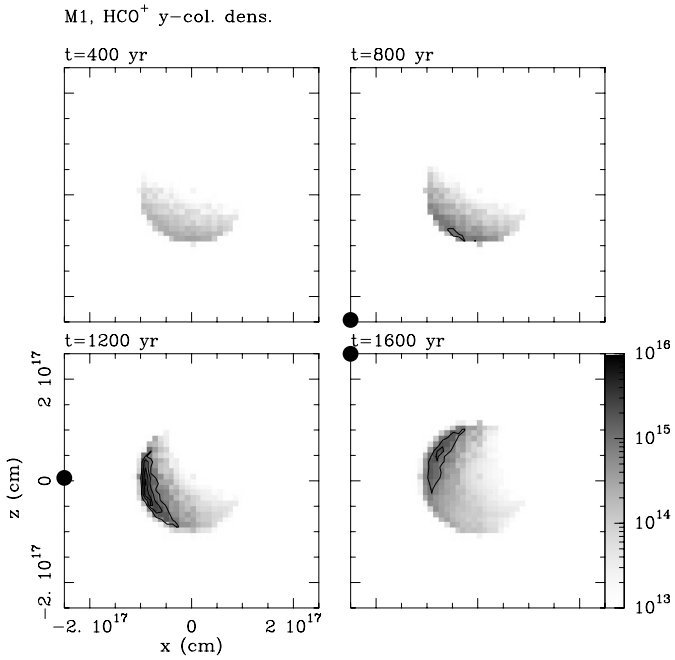

Fig. 4. Column densities (cm^{-2}) of HCO^+ through the clump integrated along lines parallel to the y-axis, at four times, for Model 1. In this orientation, the line of sight is perpendicular to the plane containing the HH trajectory and the centre of the clump. The greyscale is logarithmic, and the contours correspond to steps of 10^{15} cm^{-2}.

3.2. Model 1 – NH_3

Figs. 5–7 present results for NH_3 corresponding to those for HCO^+ in Figs. 2–4. Fig. 5 gives the fractional abundance of ammonia in the $y = 0$ plane as the source moves past the clump. In this case, no gas phase chemistry is necessary to generate the molecule, and the NH_3 in the gas phase is simply a result of photodesorption from dust grains and photodissociation by the source. The NH_3 abundances are highest within an extensive arc of the cloud, and maximum values are a few times 10^{-6}. The column density results in Fig. 6 (viewed along the x-axis) give a rather different impression from the HCO^+ results in Fig. 3, presenting an arc of emission that lags behind the source motion.

The results in Fig. 7 show a pronounced and broad arc of NH_3 column density, with values rising above 10^{16} cm^{-2} (the peak column densities as a function of time are listed in Table 3). This arc lags behind the motion of the radiation source. Its dimensions are one diameter across by about half a radius in width.

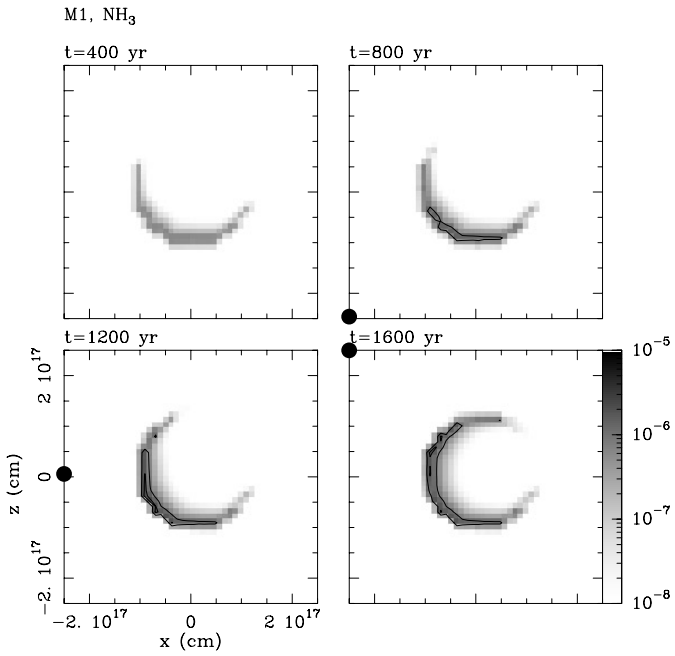

Fig. 5. As Fig. 2, for NH_3. The greyscale is logarithmic, and the contours correspond to steps of 10^{-6} in the fractional abundance.

3.3. Model 2

Since the chemistry in this scheme is driven largely by the radiation field from the HH source, it is of interest to explore the consequences of irradiation of a clump with a smaller visual extinction. In Model 2 we have adopted a visual extinction along the radius of 1 magnitude (see Table 1). Such an extinction gives a value of 2 magnitudes along a diameter, and together with a background extinction from the interclump medium will exceed the critical A_v for ice deposition (at least for clouds in Taurus; e.g., Chiar et al. 1995). We show in Figs. 8 and 9 results for the column density maps of HCO^+ and NH_3, respectively, for an orientation as in Figs. 4 and 7. Evidently, the radiation field

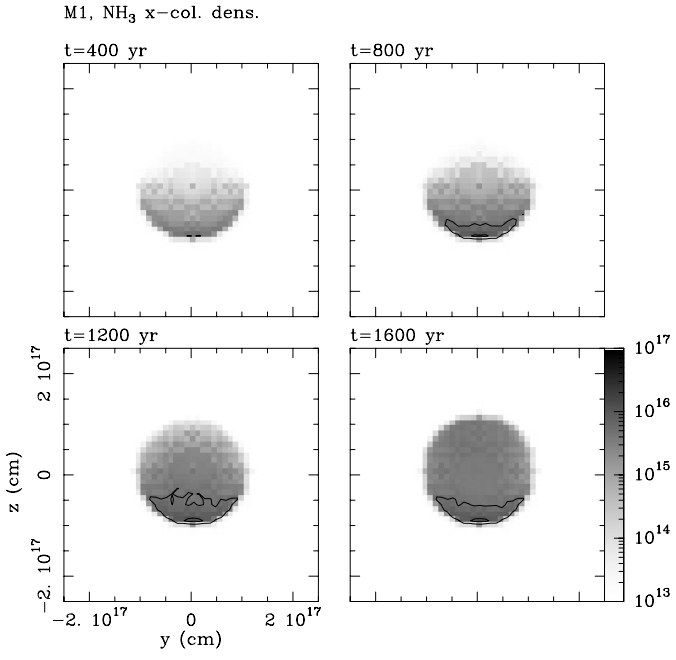

Fig. 6. As Fig. 3, for NH_3. The greyscale is logarithmic, and the contours correspond to steps of 2×10^{15} cm^{-2}.

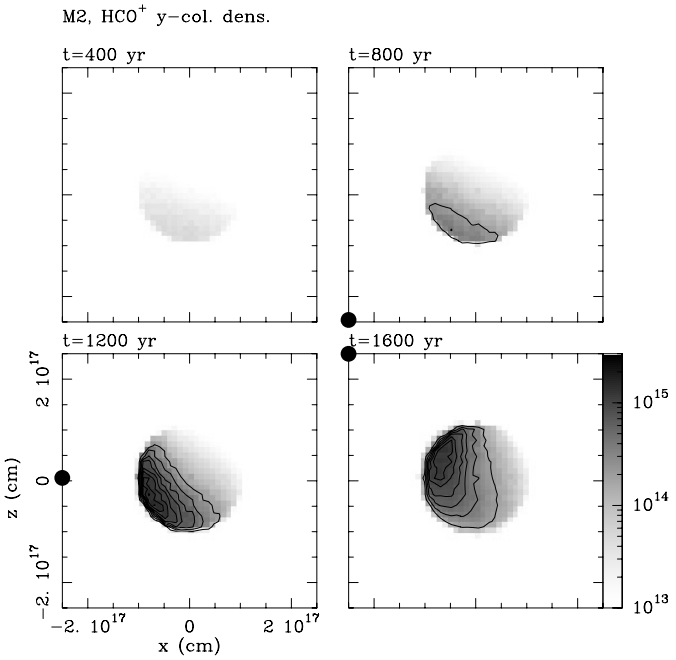

Fig. 8. Column densities (cm^{-2}) of HCO^+ through the clump integrated along lines parallel to the y-axis, at four times, for Model 2. In this orientation, the line of sight is perpendicular to the plane containing the HH trajectory and the centre of the clump. The greyscale is logarithmic, and the contours correspond to steps of 2×10^{14} cm^{-2}.

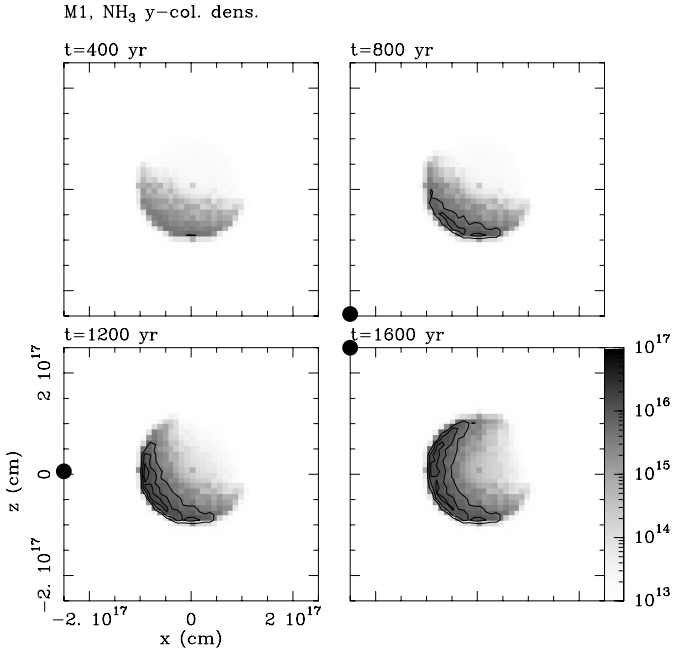

Fig. 7. As Fig. 4, for NH_3. The greyscale is logarithmic, and the contours correspond to steps of 10^{15} cm^{-2}.

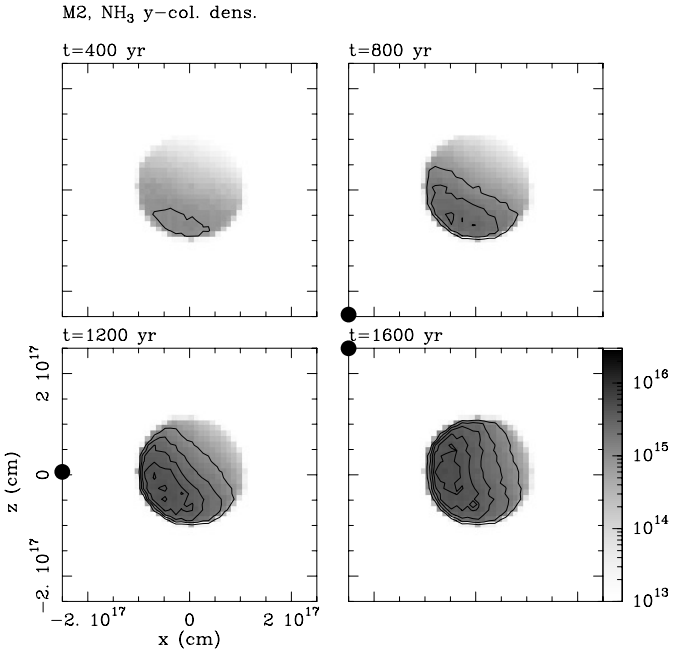

Fig. 9. As Fig. 8, for NH_3. The greyscale is logarithmic, and the contours correspond to steps of 10^{15} cm^{-2}.

penetrates the clump to a much greater extent than in Model 1, and the consequent chemistry is more spatially extensive; the column densities are in general comparable, the regions of emission are more extensive, and the arcs are broader and more like bars, with an aspect ratio of about 2.

3.4. Molecules in the dust

The efficiency for desorption of molecules from the dust grains has been set at a low value in the calculations presented. We have obtained results for the amount of any species remaining

Table 3. Column densities (in units of 10^{15} cm^{-3}) integrated along the y-axis

t (yr)	Model 1		Model 2	
	HCO^+	NH_3	HCO^+	NH_3
400	0.32	5.34	0.05	1.22
800	1.05	1.15	0.41	3.12
1200	4.18	17.8	1.61	5.16
1600	1.97	17.3	1.37	5.62

on the dust at any time. These results show that relatively small amounts of the mantle ices are needed to drive the chemistry that is explored here. Even at the latest time illustrated in the figures, most of the H_2O ice remains intact over the more shielded portion of the clump, for Model 2. In a shell corresponding to the region of high HCO^+ abundance, the H_2O ice abundance is reduced by up to one half. At 1600 years' evolution then nearly all NH_3 has been removed over a volume of about one half of the sphere. This corresponds precisely to the region in which NH_3 is predicted to be abundant in the gas, where it becomes subject to photodestruction.

4. Discussion

This investigation extends the earlier studies of Taylor & Williams (1996) and Viti & Williams (1999) of the impact of HH radiation on evolved clumps in a molecular cloud into which the HH object is penetrating. In the present study, the time dependence of the radiation field from the bypassing HH object is explicit, and the morphology of the emission regions for HCO^+ and NH_3 is described for the case of an initially spherical clump.

One important conclusion of this study is that the clump is structurally unchanged by the passage of a nearby HH object. The 3-D code employed included heating and cooling processes and was capable of following the evaporation of the clump into the ambient medium. It was found that evaporation velocities were essentially zero, within the accuracy of the code, and that during the evolution the clump temperature and density remained very close to their initial values. The impact parameter of the HH path and the clump was chosen to be 2.5 times the clump radius. A reduction to one radius would enhance the heating effect by about an order of magnitude but the cooling processes would still ensure that the temperature and pressure would not be significantly changed. Direct impact of the shock on the clump is beyond the scope of this paper, but would of course generate very high temperatures and pressures within the clump, and ultimately clump disruption. The case of direct impact will be investigated in a later paper.

The shock velocity adopted, 200 km s^{-1}, is already large and is near the upper end of the range of values observed. Therefore, it is unlikely that the radiation field intensity on the clump will be significantly larger than the value adopted here. We conclude that in an indirect impact the clump is likely to survive essentially unchanged physically. However, as the present work emphasises, the clump is changed chemically to a significant extent.

The chemical study contained in this work deliberately restricts the chemistry to the two species, HCO^+ and NH_3, for which enhancements near HH objects were first observed. The restriction was made to enable rapid computation of different models. The results are qualitatively similar to those obtained earlier for the assumed static radiation field case. The new information provided by this work is the predicted detailed structure that should arise from a spherical clump viewed in particular orientations with respect to the line of passage of the HH object. The general result is that the morphologies of molecular line emission arising from a spherical clump in this situation could be observed as ranging from roughly spherical (though smaller than the clump size) to arc-like, depending on the orientation of viewing of the clump. In the case viewing perpendicular to the plane containing the HH velocity and the clump centre, then the morphology is arc-like, and the position of the radiation source will be on the outside of the arc and beyond one end of it. However, the optical depth within the clump has a significant effect on the shape of the arcs. For low optical depths, the arcs become broader and more bar-like. Where the line of sight places the HH velocity line behind the clump, then the morphologies are uninformative "blobs". However, the position of these blobs should move within the clump on a timescale of the passage time. For a relatively nearby object, e.g. in Taurus, this is equivalent to a detectable proper motion of a few tenths of an arcsec per year.

These structures are likely to persist for significantly long times. The timescale for chemical change by cosmic ray ionisation is about one million years, but penetration of the interstellar radiation field into the clump will introduce chemical changes on a timescale that is about one order of magnitude smaller. Therefore, we expect deviations from the chemical structures predicted here to begin to appear after about 3×10^4 years. One implication of this conclusion is that the association of an enhancement in NH_3 and HCO^+ with an HH object need not necessarily imply that the HH object is the cause of that enhancement; the enhancement may be a result of a previous outburst, within a few tens of thousands of years.

There are a number of HH objects where high resolution maps have been made in lines of HCO^+ and NH_3. Girart et al. (1994) mapped ammonia emission associated with HH80 North, and downstream from it. The morphology of the emitting region is unclear. There is a resolved, roughly circular blob, that may have some unresolved extensions. If these are taken to form an arc, then that arc cannot be interpreted as arising from the presence of HH80 N on the basis of the present model, because its curvature is in the wrong sense with respect to the HH velocity. However, the central blob could be interpreted as the morphology of a spherical core that is nearly in the line of sight to HH80 N. The HCO^+ observations (Girart et al. 1998) have even poorer resolution, but they also indicate a roughly circular (projected) blob that may be slightly displaced from the ammonia peak. This displacement is in the sense expected from the models presented here, i. e. that the ammonia emission is centred closer to the HH object. This source is further complicated, however, by the presence of an IRAS source with positional error bars encompassing the ammonia emission, and it cannot be

ruled out that the ammonia emission could be associated with a young star at that position.

Torrelles et al. (1993) mapped NH_3 emission towards HH1 and found a variety of structures. This region is also complicated, in this case by the presence of a nearby maser, which implies high excitation. Some NH_3 emission appears to be associated with the maser. Some of the rest may be roughly spherical but somewhat extended in the line of the HH velocity. The radiation sources may be the optical knots identified by Raga et al. (1990) which are roughly centrally located with respect to the clump. If so, then the jet and the clump are in the same line of sight.

Torrelles et al. (1992) mapped ammonia emission towards HH2 and found an arc-like structure near to the optical knots identified by Raga et al. (1990). This arc is suggestive of the structures predicted from the present model. However, the orientation of the arc is incompatible with the present position of the optical knots. It is possible, however, that the ammonia was caused by a previous outburst from the star, along the same path. We have, therefore, run models in which a second outburst is presumed to occur on the same path. We find that the passage of a second HH object produces an enhancement in the NH_3 and HCO^+ column densities of up to a factor of 2. This is result is consistent with the fact (see Sect. 3.4) that only a relatively small amount of the ice is removed during the first passage of an HH object.

Acknowledgements. DAW is grateful for hospitality at the IAUNAM, where this work was carried out. He also acknowledges with thanks the support of a PPARC Senior Fellowship. The work of AR was partially supported by the CONACyT grants 26833-E and 27546-E and the DGAPA (UNAM) grant IN109297. We would like to thank Guillaume Pineau des Fôrets (the referee) for very helpful comments about the paper.

References

Allen M., Robinson G.W., 1975, ApJ 195, 81
Bakes E., Tielens A.G.G.M., 1994, ApJ 427, 822
Chiar J.E., Adamson A.J., Kerr T.H., Whittet D.C.B., 1995, ApJ 455, 234
d'Hendecourt L., Allamandola L.J., Baas F., Greenberg J.M., 1982, A&A 109, L12
Dzegilenko F., Herbst E., 1994, J. Chem. Phys. 100, 9205
Dzegilenko F., Herbst E., 1995, ApJ 443, L81
Dzegilenko F., Herbst E., Uzer T., 1995, J. Chem. Phys. 102, 2593
Girart J.M., Rodríguez L.F., Anglada G., et al., 1994, ApJ 435, L145
Girart J.M., Estalella R., Ho P.T.P., 1998, ApJ 495, 59
Launay J.M., Roueff E., 1977, A&A 56, 289
Léger A., Jura M., Omont A., 1985, A&A 144, 147
McKee C.F., Storey J.W.V., Watson D.M., Green S., 1982, ApJ 259, 647
Millar T.J., Farquhar P.R.A., Willacy K., 1997, A&AS 121, 139
Monteiro T.S., Flower D.R., 1987, MNRAS 228, 101
Raga A.C., Barnes P.J., Mateo M., 1990, AJ 99, 1912
Raga A.C., Wang L., 1994, MNRAS 268, 354
Raga A.C., Mellema G., Arthur S.J., et al., 1999, Rev. Mex. Astron. Astrofis. 35, 123
Rudolph, A., Welch W.J., 1988, ApJ 326, L31
Taylor S.D., Williams D.A., 1996, MNRAS 282, 1343
Torrelles J.M., Rodríguez L.F., Cantó J., et al., 1992, ApJ 396, L95
Torrelles J.M., Gómez J.F., Ho P.T.P., et al., 1993, ApJ 417, 655
Van Leer B., 1982, ICASE report No. 82-30
Viti S., Williams D.A., 1999, MNRAS 310, 517
Westley M.S., Baragiola R.A., Johnson R.E., Baratta G.A., 1995, Nat 373, 405
Willacy K., Williams D.A., 1993, MNRAS 260, 635
Wolfire M.G., Königl A., 1991, ApJ 383, 205
Wolfire 2M.G., Königl A., 1993, ApJ 415, 204